Supplement of Biogeosciences, 16, 3543–3564, 2019
https://doi.org/10.5194/bg-16-3543-2019-supplement

Biogeosciences Open Access EGU

Supplement of

Particulate organic matter controls benthic microbial N retention and N removal in contrasting estuaries of the Baltic Sea

Ines Bartl et al.

Correspondence to: Ines Bartl (ines.bartl@io-warnemuende.de)

Supplements

Table S1: Overview of new and recently published environmental data and process rates used for comparison of the contrasting Vistula and Öre estuaries in this study.

Variables	----------Öre estuary----------		----------Vistula estuary----------		
	Hellemann et al., 2017	this study	Bartl et al., 2018	Thoms et al., 2018	this study
Salinity	x		x		
Temperature	x		x		
Oxygen	x	x	x		
DIN		x	x		
Chl.*a*		x			x
POC	x		x		
^{13}C-POC	x				x
PON	x		x		
C:N	x		x		
POC:Chl.*a*		x			x
Sediment type	x			x	
Porosity	x				x
LOI	x			x	
Permeability	x				x
OPD	x				x
Pore-water NH_4^+ concentrations		x		x	
Pore-water NH_4^+ pools		x			x
Nitrification rate		x	x		
NH_4^+ assimilation rate					
Denitrification rate	x				x

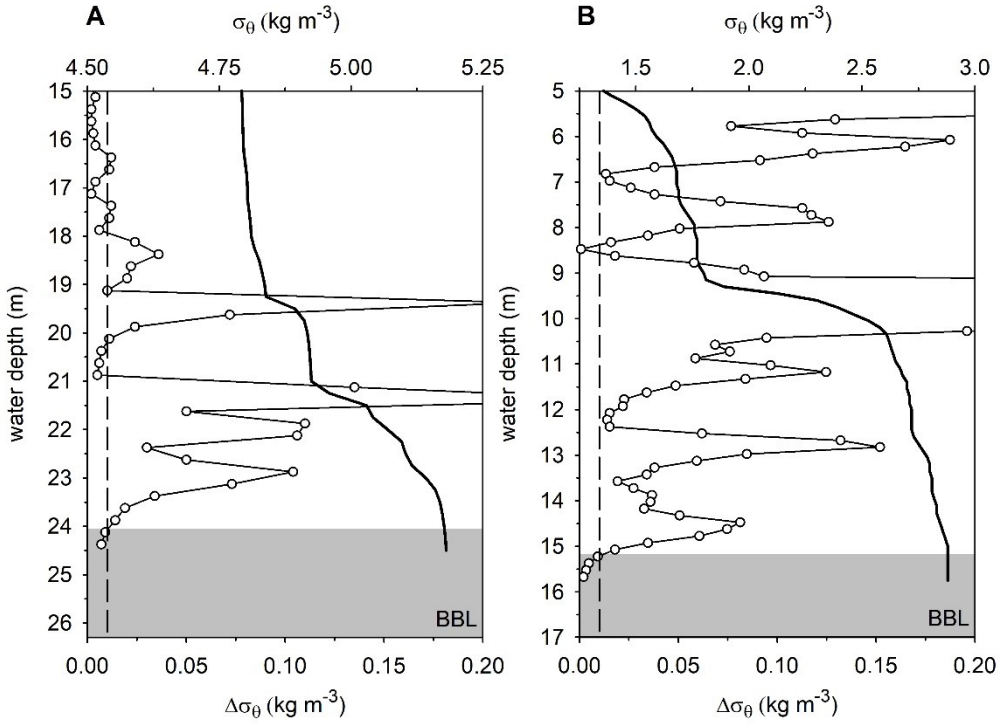

Figure S1: Vertical profiles of the potential density σ_θ (black thick line) and the variation of the potential density $\Delta\sigma_\theta$ (white circles) of station VE05 from the Vistula estuary (A) and N3 from the Öre estuary (B). The threshold of the change of potential density ($\Delta\sigma_\theta$) at 0.01 kg m^{-3} is indicated by the dashed line. The vertical extent of the bottom boundary layer (BBL) is the difference between the bottom depth and the depth at which $\Delta\sigma_\theta$ exceeds the threshold (grey box).

Table S2: Environmental variables in river, river plume, estuarine surface layer (where no river plume signal was found), mid- and bottom boundary layer (BBL) of the Öre and Vistula estuaries in spring and summer. Values given as average and standard deviation of each water layer, number of samples in parentheses, missing data noted as 'not available' (n.a.) or 'not detectable' (n.d.). For the water lavers river, river plume, estuarine surface and mid water ranges of the sampling depths are shown, while for the BBL the ranges of vertical extents from the seafloor are given.

Site	Season	Water layer	Range of sampling depth/ BBL extent	Salinity	Temperature	Oxygen	$NO_3^-+NO_2^-$	NH_4^+
			m		°C	µmol L^{-1}	µmol L^{-1}	µmol L^{-1}
Öre estuary[a]	Spring	River	0	0	3	n.a.	6	0.7
		River plume	0-1	1.7 ± 1.2 (12)	4.7 ± 1.0 (12)	316.2 ± 46.7 (7)	5.1 ± 2.7 (12)	0.3 ± 0.2 (12)
		Est Surface	0-1	4.3 ± 0.8 (19)	4.1 ± 0.6 (19)	328.1 ± 32.6 (9)	0.6 ± 0.5 (14)	0.1 ± 0.1 (17)
		Mid	3-20	4.6 ± 0.6 (18)	3.5 ± 0.4 (18)	377.3 ± 21.6 (11)	0.7 ± 0.6 (16)	0.2 ± 0.2 (16)
		BBL	2-3.9	5.0 ± 0.4 (12)	2.8 ± 0.1 (12)	389.3 ± 19 (4)	2.4 ± 1.2 (11)	0.3 ± 0.3 (13)
	Summer	River	0	0	17.5	n.a.	0.6	0.3
		River plume	0-1	1.4 ± 0.6 (7)	17.0 ± 0.4 (7)	292.7 ± 2.6 (8)	0.7 ± 1.3 (9)	0.2 ± 0.1 (11)
		Est. Surface	0-1	2.8 ± 0.2 (18)	16.5 ± 0.5 (18)	302.6 ± 5.2 (18)	0.1 ± 0.1 (5)	0.1 ± 0.0 (17)
		Mid	4-15	3.2 ± 0.5 (22)	14.3 ± 1.2 (22)	280.0 ± 10.1 (23)	0.3 ± 0.2 (9)	0.2 ± 0.1 (22)
		BBL	1.2-2.6	4.5 ± 0.6 (6)	7.4 ± 0.8 (7)	237.63 ± 14.0 (7)	2.3 ± 0.6 (9)	1.1 ± 0.6 (9)
Vistula estuary[b]	Spring	River	0	0.2	3.9	n.a.	286.96	6.67
		River plume	0-2	3.6 ± 1.7 (6)	4.1 ± 0.3 (6)	387.9 ± 9.9 (6)	152.2 ± 80.4 (8)	3.5 ± 2.5 (8)
		Est. Surface	0-2.5	6.9 ± 0.4 (6)	4.2 ± 0.2 (6)	405.1 ± 21.2 (6)	21.7 ± 13.8 (6)	0.3 ± 0.2 (6)
		Mid	10-20	7.6 ± 0.1 (18)	4.2 ± 0.1 (18)	376.1 ± 13.7 (18)	5.0 ± 1.6 (9)	0.3 ± 0.1 (8)
		BBL	3.2-6.9	7.7 ± 0.3 (19)	4.1 ± 0.2 (9)	355.8 ± 11.0 (17)	5.9 ± 1.5 (19)	0.6 ± 0.3 (18)
	Summer	River	0	n.a.	n.a.	n.a.	n.a.	n.a.
		River plume	1.25	6	20.8	398	n.d.	0.5
		Est. Surface	0-2	6.9 ± 0.2 (7)	16.7 ± 1.3 (7)	312.2 ± 27.9 (7)	n.d.	0.2 ± 0.1 (7)
		Mid	10-20	7.3 ± 0.1 (14)	14.3 ± 0.7 (14)	276.8 ± 18.9 (14)	0.4 ± 0.4 (5)	0.4 ± 0.3 (14)
		BBL	1.4-6.7	7.7 ± 0.2 (7)	8.2 ± 3.4 (7)	263.2 ± 17.9 (7)	1.0 ± 0.8 (13)	3.5 ± 2.0 (13)

[a] Salinity, Temperature and BBL oxygen from Hellemann et al. (2017)
[b] Data from Bartl et al. (2018)

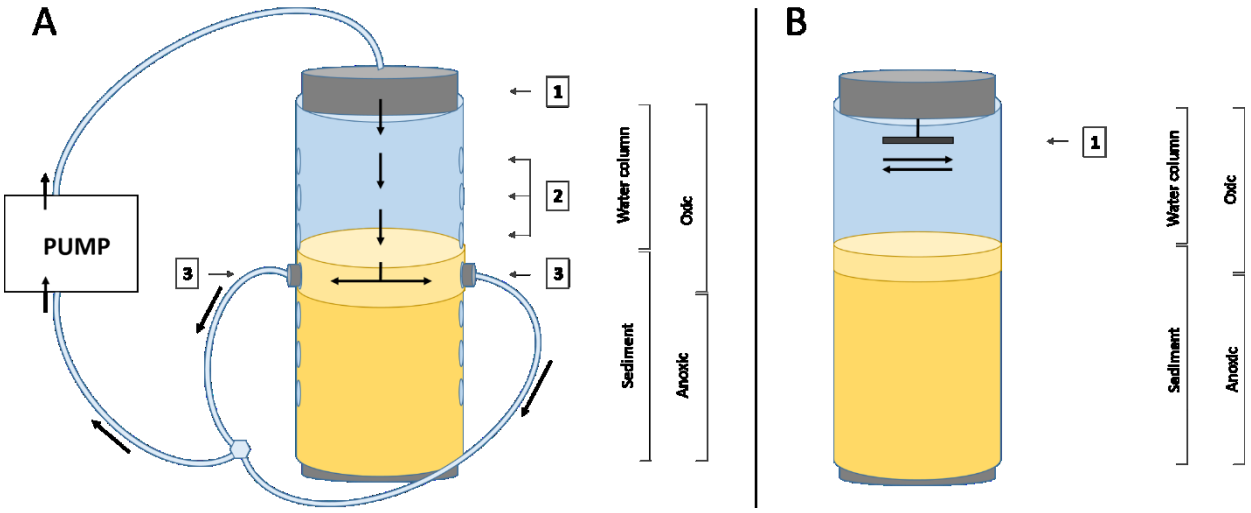

Figure S2: A schematic of the incubation design used to measure N_2 production in (A) permeable sediments with advective pore-water flow and (B) sediments under diffusive water motion. A: Site-water spiked with $^{15}N\text{-}NO_3^-$ tracer is pumped into the core from the top (1) and drawn out again through the advective, oxic sediment layer (3), identified from the oxygen profiles. The outflow ports have a resolution of 5 mm and can be adjusted (2), depending on the sediment height in the core and the depth of the advective layer. B: Isotopic tracer is added to the water column of the incubation core and thereafter distributed by diffusion, which is aided by gentle water motion from a magnetic stirrer (1).

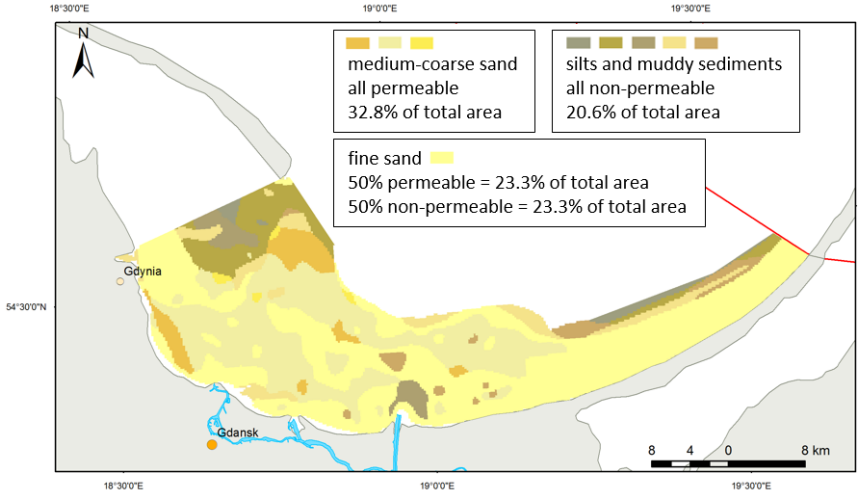

Figure S3: Sediment types of the Vistula estuary. For the fine sands, a permeable and a non-permeable character was used in a 1:1 ratio, as roughly half of all samples from this sediment type were permeable. Sediment map provided by Halina Kendierska (University of Gdansk). Total estuarine area (825 km^2) and areal proportions of the sediment types were calculated by Mayya Gogina (Leibniz-Institute for Baltic Sea Research Warnemünde).

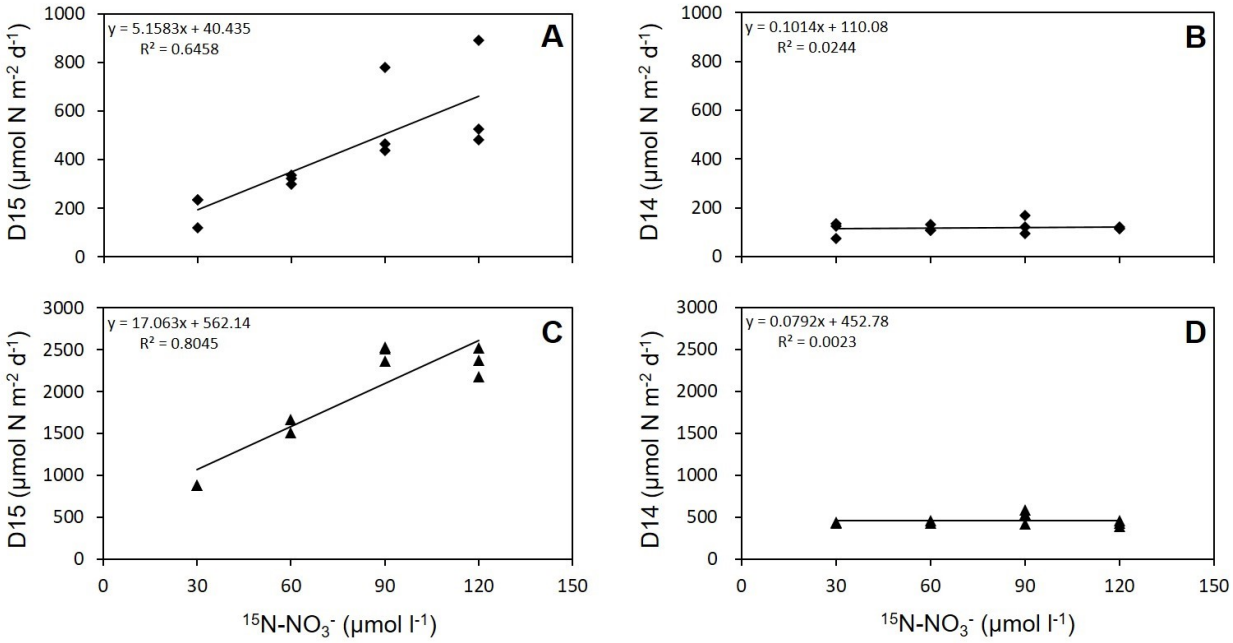

Figure S4: Example plots of regression analyses which were performed with all N_2 data (A, B = Öre Estuary, station N34; C, D = Vistula Estuary, station VE05; both summer). Plots show that D15 (= the denitrification of $^{15}N\text{-}NO_3^-$) increases with increasing tracer concentration (A, C), fulfilling requirements of IPT (Nielsen 1992), and that D14 (= the true denitrification) does not increase with increasing tracer concentration (B, D), indicating that annamox did not contribute to total N_2 production (Risgaard-Petersen et al. 2003).

S1 Estimation of the absence / presence of advective pore-water flow in the permeable sediment of the Vistula estuary

Theoretical pressure gradients at the sediment surface, established based on the interaction of near-bottom flow with sediment topography, were estimated for the sampling period (July 05–11, 2014) using a theoretical topographical object (sediment mound) with a height of 3 cm and model-derived near-bottom flow velocity (average and maximum, Table 2) derived by using the General Estuarine Transport Model (GETM; for further details see Holtermann et al., 2014). This model has been thoroughly tested for applications in the Baltic Sea (e.g. Burchard et al., 2009, 2005). The modelled bottom flow velocity was derived from 50 cm above the sediment; hence, the actual near-bottom flow velocity is probably lower due to increasing friction with decreasing distance to the sediment.

The theoretical horizontal pore-water flow over a distance of 1 cm was calculated after Bear (1972), using the estimated pressure gradients from Figure 4 in Huettel et al. (1996) and equations derived from Darcy´s Law together with the average measured hydraulic conductivity, water density and porosity. The Peclet number, an indicator of the dominating transport mechanism in the sediment, was calculated by dividing the pore-water flow velocity by the diffusive transport velocity. We used oxygen as example element to be transported over 1 cm distance by molecular diffusion in the sediment (calculated after Schulz 2005), with period-specific salinity and porosity at 20°C to allow comparisons with hydraulic conductivity measurements). A Peclet number ≥ 5 indicates the dominance of advective processes over diffusive processes (Bear, 1972 and references therein).

Table S3: Estimation of the pressure gradient at the sediment surface, the resulting pore-water (PW) flow velocity, and the Peclet number (output variables) in the permeable sediment of the Vistula estuary, based on a modeled bottom-water (BW) flow velocity 50 cm above the sediment surface, the height of a representative topographic object, and the molecular diffusion of oxygen, as an example element (input variables); averages and the maximum values in parentheses.

	Input variables			Output variables		
Period	**BW flow velocity** (cm s^{-1})	**Object height** (cm)	**Molecular diffusion** (10^{-6} cm s^{-1})	**Pressure gradient** (Pa)	**PW flow velocity** (10^{-6} cm s^{-1})	**Peclet Nb**
05.–11.07.2014	1.4 ± 0.2 (2.5)	3.0	7.27	< 0.10 (0.15)	15.20 (22.81)	2.1 (3.1)

References in the supplements

Bartl, I., Liskow, I., Schulz, K., Voss, M. and Umlauf, L.: River plume and bottom boundary layer – Hotspots for nitrification in a coastal bay?, Estuar. Coast. Shelf Sci., 208, 70–82, doi:10.1016/j.ecss.2018.04.023, 2018.

Bear, J.: Dynamics of fluids in porous media, American Elsevier Pub. Co, New York, NY., 1972.

Burchard, H., Lass, H. U., Mohrholz, V., Umlauf, L., Sellschopp, J., Fiekas, V., Bolding, K. and Arneborg, L.: Dynamics of medium-intensity dense water plumes in the Arkona Basin, Western Baltic Sea, in Ocean Dynamics, vol. 55, pp. 391–402, Springer-Verlag., 2005.

Burchard, H., Janssen, F., Bolding, K., Umlauf, L. and Rennau, H.: Model simulations of dense bottom currents in the Western Baltic Sea, Cont. Shelf Res., 29(1), 205–220, doi:10.1016/j.csr.2007.09.010, 2009.

Hellemann, D., Tallberg, P., Bartl, I., Voss, M. and Hietanen, S.: Denitrification in an oligotrophic estuary: A delayed sink for riverine nitrate, Mar. Ecol. Prog. Ser., 583, 63–80, doi:10.3354/meps12359, 2017.

Holtermann, P. L., Burchard, H., Gräwe, U., Klingbeil, K. and Umlauf, L.: Deep-water dynamics and boundary mixing in a nontidal stratified basin: A modeling study of the Baltic Sea, J. Geophys. Res. Ocean., 119(2), 1465–1487, doi:10.1002/2013JC009483, 2014.

Huettel, M., Ziebis, W. and Forster, S.: Flow-induced uptake of particulate matter in permeable sediments, Limnol. Oceanogr., 41(2), 309–322, 1996.

Schulz, H. D.: Quantification of Early Diagenesis: Dissolved Constituents in Marine Pore Water, in Marine Geochemistry, pp. 85–128, Springer, Berlin, Heidelberg., 2013.